Muscle Control Algorithm to Simulate Voluntary Head-Neck Movements during Avoidance Manoeuvres using an Occupant Active Human Body Model

María González-García, Jens Weber, Baptiste Sandoz, Steffen Peldschus

Abstract Vehicle occupant posture might change due to avoidance manoeuvres, such as braking or lane change, that occur prior to a potential collision. This deviation from the initial posture can compromise the effective engagement of the safety systems with the occupant, which may result in a different injury outcome. It is therefore important to have a tool to predict occupant kinematics during pre-crash manoeuvres in order to improve and develop safety systems that take this change in posture into account. Active Human Body Models are virtual tools with muscle control algorithms which can predict the kinematics of vehicle occupants. However, these models generally are able to execute limited voluntary movements that can affect the posture, such as head-neck movements. This study proposes three additional controllers to the reflexive control that enable voluntary extension and lateral bending of the head, which has been exercised with the THUMS TUC-VW AHBM. The muscle control is also capable of representing two different activation levels, namely *low* and *highly tensed*. The model kinematics were compared with corridors from volunteer experimental data, for braking and lateral acceleration load cases. The model's performance was improved in all cases by the incorporation of the voluntary muscle control.

Keywords Active Human Body Model, braking, lane change, reflexive control, voluntary muscle control.

I. INTRODUCTION

Active Human Body Models (AHBMs) are virtual finite element (FE) models used to predict the kinematics an occupant would sustain during a pre-crash manoeuvre. The resulting change in posture of the occupant during such a manoeuvre could lead to a different injury risk in the event of a vehicle collision compared to the occupant in the initial posture [1-3]. Therefore, accurate prediction of the resulting posture is of great importance in order to evaluate the performance of safety systems, taking into account the acceleration that occurs during the pre-crash phase. In contrast to the in-crash phase, the pre-crash phase, such as braking or lane-changing manoeuvres, typically lasts for 1000–2000 ms. This means the occupants have sufficient time to react to the external forces [4-7]. Parameters such as their initial muscle state or reaction time have been demonstrated to significantly influence the kinematics during such manoeuvres in volunteer experiments [8-10]. Hence, different algorithms have been implemented through the last years into several HBMs to account for muscle activation [11-21].

Most of the AHBMs use closed-loop proportional-integral-derivative controllers, with the objective of returning to their original position. However, their muscle control algorithms differ on the measurements used to regulate the level of muscle activation. While some of these AHBMs primarily regulate muscle activation based on the angular deviation of the joints [11][13][15-19], others calculate this based on the deviation of muscle length [12][14][20]. The latter method aligns with the muscle control of the central nervous system, wherein muscle spindles are responsible for measuring changes in muscle length. The combination of both methods within the muscle control algorithms for the neck musculature has been investigated in several of these AHBMs [13][16-19].

Additionally, the majority of these AHBMs react to the external acceleration with the objective of returning to its initial position; however, only a few of them are capable of performing voluntary movements. Iwamoto *et al.* [22] included supplementary muscle controllers to regulate the force exerted on the steering wheel and braking pedal. Furthermore, Martynenko *et al.* [14] investigated the usage of a hybrid controller, including an open-loop

M. González-García (e-mail: maria.gonzalez.garcia@volkswagen.de) is a Research Engineer and J. Weber is a Senior Research Engineer at Volkswagen Group Innovation, Wolfsburg, Germany. B. Sandoz is an Assistant Professor at Art et Métiers Institute of Technology, IBHGC, Paris, France. S. Peldschus is a Professor of Forensic Biomechanics at the University of Munich (LMU), Munich, Germany.

and a closed-loop controller. The open-loop controller inputs pre-optimised muscle activation curves into the muscles, which is further regulated during the simulation by the closed-loop controller. However, the kinematics of the occupant must be known in advance to apply this muscle algorithm, a prerequisite that is not typically met in the context of vehicle safety.

Yet, to the authors' knowledge, none of these AHBMs is capable of performing active head-neck movements without pre-optimised muscle activation curves. Although, previous researchers [23-25] have hypothesised that volunteers execute protective movements by laterally bending their heads during lane-changing manoeuvres when approaching the B-pillar and the side window. This assumption is founded upon the observation that head kinematics are not symmetrical during right and left lane-change manoeuvres [25], and that the head lateral excursion varies depending on the available space within the vehicle cabin, for example between a sedan and SUV [23]. Furthermore, González-García *et al.* [26] have demonstrated that there was a significant difference in the head excursion and lateral bending of volunteers on a sled subjected to lateral accelerations, when a lateral structure was or was not placed on the side of the volunteer, representing the frame of a sedan vehicle.

The aim of the present study was to incorporate additional muscle controllers for the neck musculature in order to predict voluntary protective movements during braking and lane-changing manoeuvres. Specifically, the development of these muscle control algorithms has been implemented into the THUMS TUC-VW AHBM.

II. METHODS

The THUMS TUC-VW AHBM [1][12][27] in the Virtual Performance Solution (VPS) (ESI Group, Keysight, Bagneux, France) solver is applied as the baseline in this investigation. This model is based on the passive THUMS TUC 2020, which, in turn, is based on the 50th percentile male THUMS version 3 [22]. The THUMS TUC-VW AHBM includes a total of 600 muscles, modelled with 1-D Hill-type elements. Each muscle is divided into multiple bar elements to represent the curved muscle path. Additionally, the original material properties of the soft tissues of the THUMS TUC have been modified [12][27] according to literature data [28-31].

Volunteer Experimental Data for Validation

Two different validation datasets, including volunteers with anthropometry comparable to that of a 50th percentile American male, were selected to validate the THUMS TUC-VW AHBM under low g frontal and lateral accelerations.

The first validation dataset, reported by Huber *et al.* [4], comprised data from 19 male volunteers (178.2 ± 5.0 cm, 77.8 ± 8.4 kg). The volunteers were seated on a modified production seat of a Mercedes-Benz S500 vehicle, in which the foam cushion was replaced by a wooden plate with 40 mm of foam padding (N5063), covered by artificial leather. Each volunteer was subjected to multiple pulses. The present study utilised the data from the braking pulse, with a maximum deceleration of 1 g for 1.5 s at an initial velocity of 50 km/h. The kinematics of the THUMS TUC-VW AHBM were compared with the volunteers' forward head and thoracic excursion as well as head flexion corridors. Additionally, the comparison with the shoulder seat-belt forces can be found in Appendix A.

In the second validation dataset, the THUMS TUC-VW AHBM was compared with the data from 10 male volunteers (176.6 ± 2.9 cm, 75.8 ± 3.0 kg) subjected to lateral accelerations on a sled [9][26]. The volunteers were seated on a wooden plate with their feet placed on a footrest and secured by a thigh belt. The volunteers were subjected to multiple acceleration pulses, each of which was repeated three times. In this study, the AHBM was compared with the experimental data from the so-called *plateau high* pulse [9][26]. This pulse is characterised by two plateaus, each with a maximum of 0.3 g, corresponding to a symmetrical acceleration and deceleration phase, for a total duration of 2 s. The volunteers were also asked to either brace or to relax their muscles depending on the configuration. Moreover, for five of these volunteers an additional lateral structure was added to the sled to represent the lateral frame of a sedan vehicle type with its side window. The data from both configurations, with and without the lateral structure, were used to validate the AHBM muscle control. The kinematics of the THUMS TUC-VW AHBM were compared with the lateral excursion of the head, first (T1) and eighth (T8) thoracic vertebrae and sacrum (S1), as well as the lateral bending of the head.

Muscle Control Algorithm

The muscle control algorithm of the THUMS TUC-VW AHBM is implemented by coupling the VPS solver with the multi-domain systems software SimulationX (ESI Group, Keysight, Bagneux, France). The algorithm is divided into two muscle controls: reactive and voluntary muscle controls. The reactive muscle control activates the muscles with the objective of returning to the initial posture when the HBM is subjected to an external load. The muscle activation is calculated using a closed-loop feedback controller based on muscle lengthening and contraction velocity. The algorithm represents the response of the central nervous system to changes in muscle length generating an action potential signal through motor neurons that innervate the stretched muscles.

The stimulation of each muscle cluster is calculated applying the formula (Eq. 1) proposed by Günther *et al.* [32]:

$$STIM_i^R = \kappa_P \frac{(l_i - (1-\delta)\lambda_i + \sigma v_i}{l_{ce_{opt}}} \tag{1}$$

where, κ_P is the proportional gain, l_i is the muscle length at each timestep, $l_{ce_{opt}}$ is the optimal muscle length, δ is the static co-contraction parameter, λ_i is the target length, v_i is the contraction velocity and σ is the sensitivity to contraction velocity of the muscle.

Two sets of the parameters κ_P, δ and σ (Table I) are defined in order to capture two different muscle states with the AHBM. These two sets of parameters, referred to as *low tensed* (LT) and *highly tensed* (HT), were adjusted using a Latin hypercube design of experiments to represent the kinematics of volunteers with higher and lower muscle tension, respectively, across multiple load cases. An additional requirement for the parameter set was to ensure numerical stability.

TABLE I
REACTIVE MUSCLE CONTROL PARAMETER DEFINITION

Activation level	$\boldsymbol{\kappa_P}$	$\boldsymbol{\delta}$	σ
Low tensed	2	0.01	80
Highly tensed	10	0.01	200

In the subsequent step, the muscle activation dynamics are calculated based on the formulation proposed by Hatze [33]. The activation values are stored within a matrix and transferred to the FE AHBM once the neural delay has been attained. The neural delay is defined as follows: 30 ms for the cervical muscles; 70 ms for the trunk and upper extremity muscles; and 100 ms for the lower extremity muscles [16][34].

The 600 muscle elements are clustered into 66 muscle controller groups depending on their functionality, e.g. flexors and extensors, with the objective of reducing computational cost. The clustering scheme for the neck muscles, comprising 18 of the 66 controllers, is shown in Fig. C1 in Appendix C.

On the other hand, the voluntary muscle control activates the muscles to perform specific head-neck protective movements. Specifically, two different movements have been incorporated into the THUMS TUC-VW AHBM: (1) extension of the neck during frontal accelerations with the objective of maintaining the view on the road; and (2) lateral bending of the neck as a protective movement to prevent contact with the lateral frame of the vehicle. The additional controllers implemented to achieve these voluntary movements are based on the human sensory systems considering the proprioceptive system for the lengthening of the muscles, the vestibular system for detecting the direction of the movement, and the visual system to estimate the distance to the surrounding environment (Fig. 1). To this end, multiple sensors have been incorporated into the AHBM. In addition to the muscle sensor, which has been previously described and which is applied in the same way as for the reactive controller, the AHBM incorporates two sensors to measure the rotational acceleration in the sagittal plane and linear acceleration in the frontal axis of the head at the centre of gravity (COG), a sensor to measure the deviation of the head-neck angle with respect to its initial position, and a sensor to measure the distance between the head and a lateral structure, such as the door-frame of a vehicle. The latter sensor is used for calculating the minimum distance between the head COG and the nodes from selected parts from the vehicle structure.

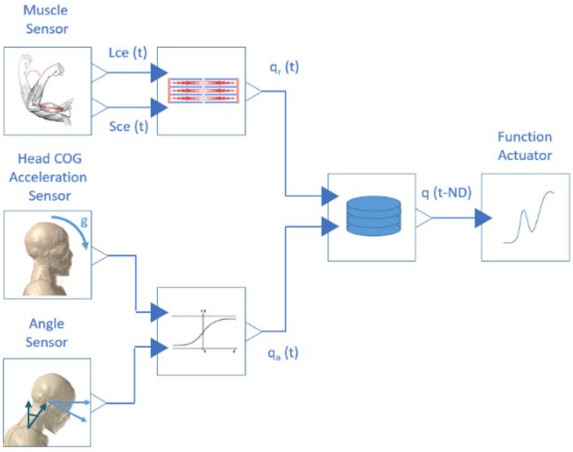

(a) Voluntary neck extension under frontal accelerations.

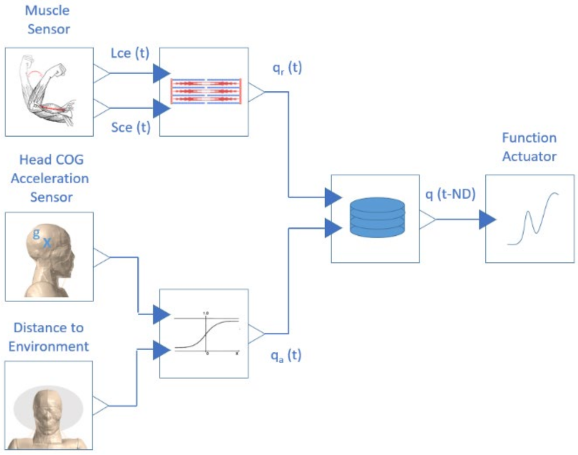

(b) Voluntary neck unilateral bending under lateral accelerations.

Fig. 1. Schema of the voluntary head-neck muscle control algorithm.

The voluntary extension of the head is initiated in the event of a rotational acceleration, resulting from flexion of the head, in conjunction with a deviation of the head-neck angle of more than 5° from its initial position. The head-neck angle deviation is determined by measuring the angle formed between the initial Frankfurt plane and the plane itself at each time step, along with the change in the vector angle of the first cervical (C1) and first thoracic vertebrae from its initial position (Fig. 1(a)). The definition of C1 and T1 landmarks was based on the COG of the body of the respective vertebra. If the Frankfurt plane angle deviates by more than 5° from its initial position, the Rectus Capitis muscle group is activated. Conversely, if the C1-T1 angle deviates from its initial orientation, the voluntary control will regulate muscle groups like the Semispinalis Capitis and Splenius Cervicis. The stimulation for the voluntary control is determined based on the firing rate of the motor neurons, which can be estimated by a sigmoid function (Eq. 2) [35]:

$$STIM_i^V = \frac{1}{1 + exp^{-S*w_i+B}} \tag{2}$$

where, S and B are muscle control parameters and w_i is the deviation of the head-neck angle.

Subsequently, the voluntary muscle activation is calculated based on the Ca^{2+} release following the formulation by Hatze [33], in the same way as was done to determine the reactive muscle activation.

TABLE II
VOLUNTARY MUSCLE CONTROL PARAMETER DEFINITION

Activation level	**Muscle control**	***S***	***B***
	Extension OC	0.3	5
Low tensed	Extension C1-T1	0.1	5
	Lateral Bending	0.4	5
	Extension OC	0.7	5
Highly tensed	Extension C1-T1	0.5	5
	Lateral Bending	0.7	5

On the other hand, in the event of lateral acceleration measured at the head COG, i.e. in the frontal axis, and if the distance to the lateral frame of the vehicle is less than 30 cm, based on [26], the unilateral bending muscle control would be initiated. The initiation of this voluntary muscle control will regulate the activation of muscle groups like the Sternocleidomastoid, Scalene or Longissimus Cervicis. The determination of the voluntary stimulation is based on the firing rate of motor neurons, applying Eq. 2. In this case, w_i denotes the difference between the distance threshold and the minimum distance between the head and the lateral frame, expressed in centimetres. The corresponding antagonistic muscles are set to their basic activation level.

Finally, the reactive and voluntary muscle activations are summed, and are bounded between the basic activation and full activation levels.

The specific set of parameters for the different voluntary muscle controls and the two muscle states is presented in Table II. These parameters were adjusted in accordance with the same approach as for the reactive muscle control. To this end, a design of experiments was performed, in which the shared parameters with the reactive muscle control were kept unchanged.

Boundary Conditions for the Validation

The THUMS TUC-VW AHBM was positioned in two different FE set-ups for the purpose of validating the model against the two previously described validation load cases. In both cases, the model was repositioned to place the hands over the thighs, in accordance with the posture of the volunteers (Fig. 2(a) and Fig. 2(c)). In all simulations, the gravity load was applied for the entire duration of the simulation.

For the braking validation load case, the FE model of the seat published in [36] for the VPS solver was utilised. The seat foam material was calibrated and compared with the measurements from indentation tests [27]. A seat-belt and a footrest were integrated into the set-up in accordance with the measurements provided by Huber *et al.* [4] (Fig. 2(a)). An initial force of 10 N was defined in the seat-belt model to remove initial slack. Furthermore, its retractor was set to lock after 150 ms from the start of the simulation; this timing was determined from the seat-belt forces acquired during the experiment (Appendix, Fig. A1). The applied acceleration pulse is presented in Fig. 2(b).

The AHBM outputs were defined as described by Huber *et al* for the data from the volunteer experiments. [4]. All nodal outputs were defined in the sagittal plane. The forward excursion of the head was measured at the COG of the head; the forward excursion of the thorax was measured at the centre of the thorax at the level of the fifth thoracic vertebra.

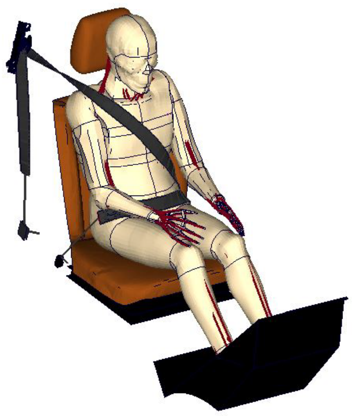

(a) FE set-up of the modified production seat with HBM for braking validation load case.

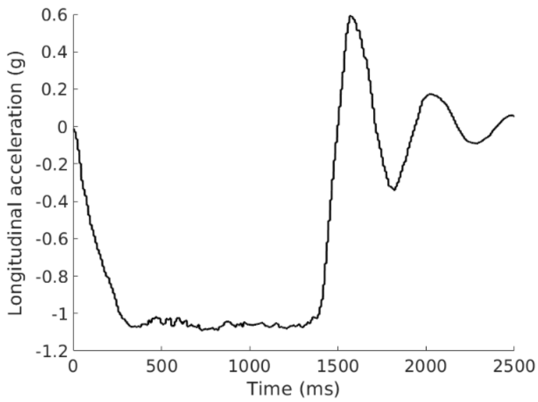

(b) Braking pulse from volunteer experiments by Huber *et al.* [4].

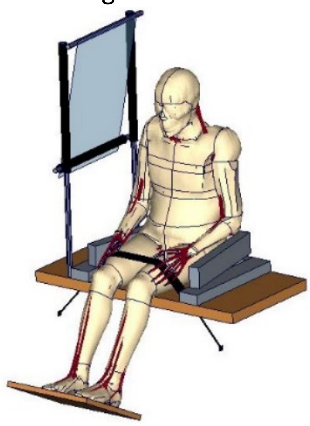

(c) FE set-up of the sled (including the lateral structure with a side window) with HBM for lateral pulse validation load case.

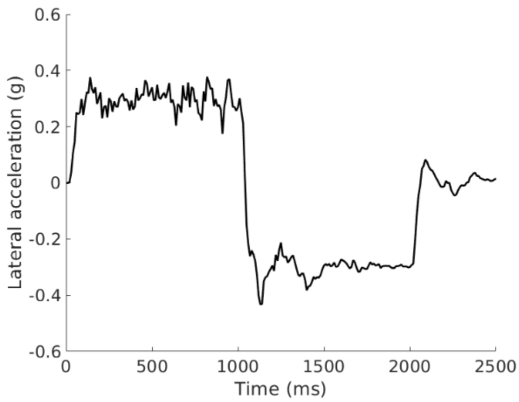

(d) Lateral pulse from volunteer experiments by Sandoz *et al.* [9] and González-García *et al.* [26].

Fig. 2. Simulation set-up for the validation of the THUMS TUC-VW AHBM under braking and lateral accelerations.

For the lateral acceleration load case, a FE model of the sled was created according to the dimensions provided by Sandoz *et al.* [9] (Fig. 2(c)). The seat plate and footrest, the aluminium pelvic profiles, and the lateral structure were defined as rigid bodies in the simulation, as the forces during this pulse are too low to deform any of these entities. The thigh seat-belt was pre-tensed with 120 N using two retractors at both ends of the seat-belt to reproduce the experimental boundary conditions. It should be noted that the lateral structure was incorporated solely into simulations that replicated the boundary conditions of the respective experimental configurations. The average lateral acceleration pulse was applied to the sled as depicted in Fig. 2(d).

The outputs in the AHBM were defined to closely match the location of the markers in the volunteer experiments. All nodal outputs were defined on the skin and in the sagittal plane. The head output was defined at the most posterior node, the T1 and T8 nodes were measured at the location of the vertebral processes on the skin, and the sacrum was defined as the node on the skin at the level of the sacral endplate.

III. RESULTS

The results of the two validation set-ups are divided into the braking and lateral acceleration subsections, below. For both validation load cases, the HBM kinematics are compared with the corridors from the volunteer responses. Each of these corridors includes the responses from all the volunteers who participated in the experiment and they are delimited by the maximum and minimum values of the curves at each time point.

Five curves are presented to depict the results of the HBM, corresponding to passive, reactive, and voluntary HBMs. For the reactive and voluntary muscle controls, both *low tensed* and *highly tensed* curves are shown. For the purpose of comparison, the excursion at 1000 ms was selected for the braking load case, as this is the time at which both, the volunteers and the HBMs, reach a stable posture. The maximum excursion during the acceleration and deceleration phases was selected in the case of the lateral acceleration load case.

Braking validation load case

Figure 3 presents the wide variation of the head kinematics exhibited by the volunteers during the 1 g braking pulse. The head forward excursion varies between 65 mm and 235 mm at 1000 ms (Fig. 3(a)). The head response of the passive HBM, without muscle activation, falls outside the range of the volunteers, reaching 295 mm forward excursion at 1000 ms. The application of the reactive muscle control reduced the head forward excursion to 230 mm and 115 mm at 1000 ms for the *low tensed* and *highly tensed* muscle activation, respectively. The voluntary muscle control further reduced the head forward excursion, reaching 202 mm and 87 mm for the *low* and *highly tensed* models, respectively. The *low tensed* and *highly tensed* curves fall within the volunteers' corridor, representing those volunteers who sustained shorter and larger head excursions.

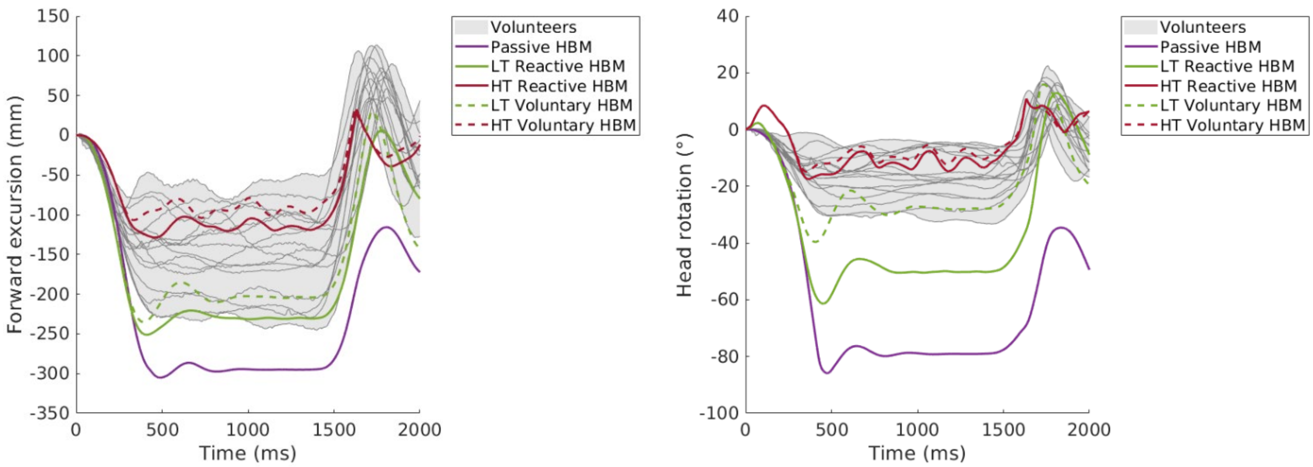

(a) Head forward excursion. (b) Head rotation in sagittal plane.

Fig. 3. Head forward excursion and rotation of the passive, reactive and voluntary muscle controls with two muscle states compared to the validation data from Huber *et al*. [4].

Similarly, Fig. 3(b) depicts the variation in head flexion among the volunteers, which ranges from 4° to 30° at 1000 ms. The passive model and the *low tensed* model, with the reactive muscle control, show larger head flexion compared to the volunteers, resulting in both curves falling outside the corridor. The application of the voluntary muscle control significantly reduced the head flexion of the AHBMs. The *low tensed* model shows a head flexion of 27°, while the *highly tensed* model exhibits a lower flexion of 7° at 1000 ms, thereby representing the volunteers with higher and lower head flexion, respectively.

The kinematic sequence of the five models is illustrated in Fig. 4, in time intervals of 250 ms up to a total of 1000 ms. As demonstrated by the curves in Fig. 3, the head flexion is substantially reduced from the passive model to those models including muscle activation, especially those incorporating the voluntary muscle control. However, for the AHBM with the *highly tensed* muscle activation level, the influence of the voluntary muscle control compared to the reactive muscle control is less significant.

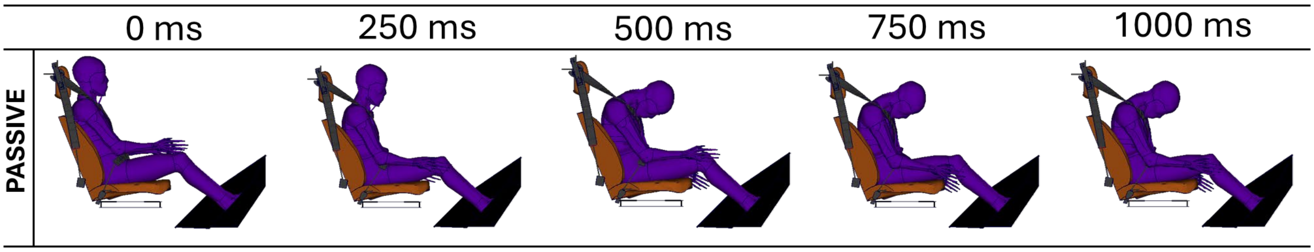

(a) Passive HBM.

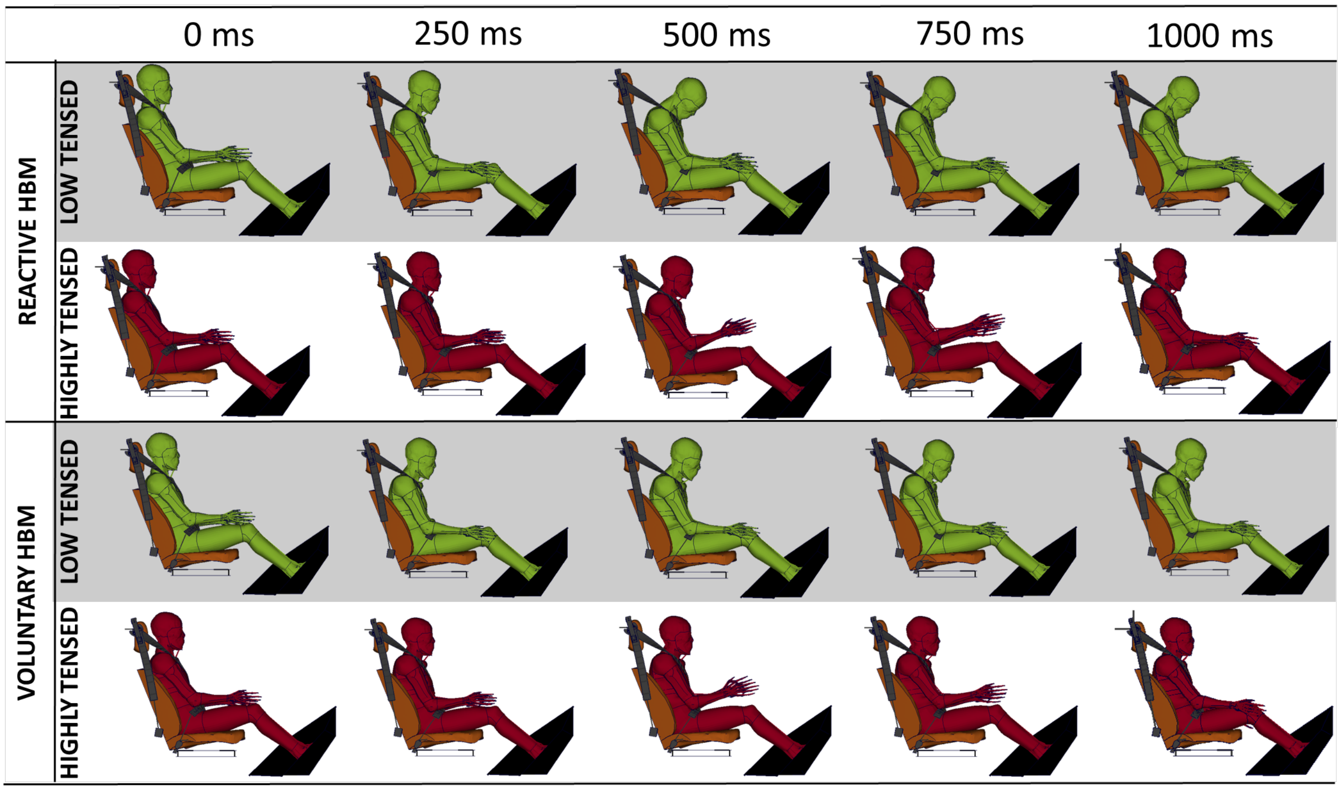

(b) Reactive and voluntary AHBM for two muscle states.

Fig. 4. Kinematic sequence of the THUMS TUC-VW HBM passive, reactive and voluntary muscle control under braking pulse from the experiments by Huber *et al*. [4].

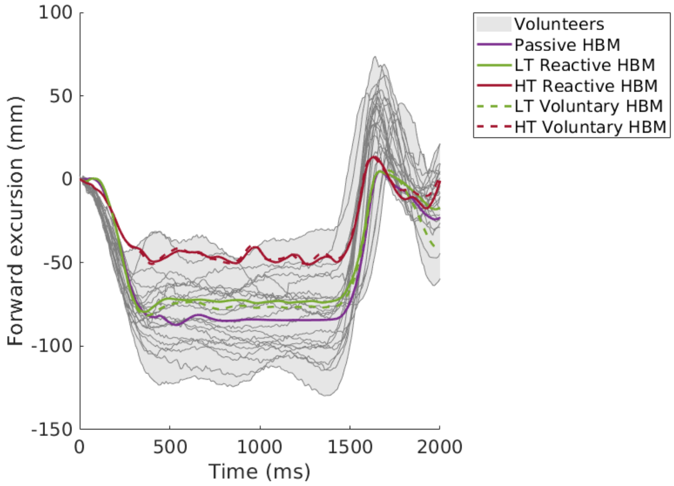

Fig. 5. Thorax forward excursion of the passive, reactive and voluntary muscle controls with two muscle states compared to the validation data from Huber *et al.* [4].

The forward excursion of the thorax among the volunteers during the 1 g braking pulse is presented in Fig. 5. The curves of the five HBMs fall within the corridor of the thorax excursion shown by the volunteers, which ranges between 40 mm and 115 mm at 1000 ms. The HBMs show a thoracic excursion of 84 mm, 74 mm and 43 mm for the passive, *low tensed* and *highly tensed* models with the reactive muscle control, respectively. The voluntary muscle control exerts a negligible influence on the thorax displacement. None of the models reveals a response similar to that of the volunteers, exhibiting larger thorax excursions, as a consequence of the shoulder-belt restraint. The *highly tensed* model shows a thorax response comparable to that of the volunteers, showing the least displacement.

Lateral acceleration validation load case

Figures 6 and 7 display the head kinematic responses of the volunteers participating in the sled volunteer experiment during a lateral pulse of up to 0.3 g acceleration. Additionally, the kinematics of T1, T8 and S1 are presented in Appendix B. Fig. 6 shows the kinematic response for the sled without the lateral structure, while Fig. 7 presents the kinematic response for the sled including the lateral structure to the right-hand side of the volunteers. It should be noted that Fig. 6 does not include the results of the AHBM with voluntary muscle control. The reason for this is that the load case has no frontal acceleration that could initiate any of the voluntary extension controllers, nor was there a lateral obstacle that could initiate the voluntary head lateral bending movement. Consequently, the results of the voluntary HBM are identical to those of the reactive HBM.

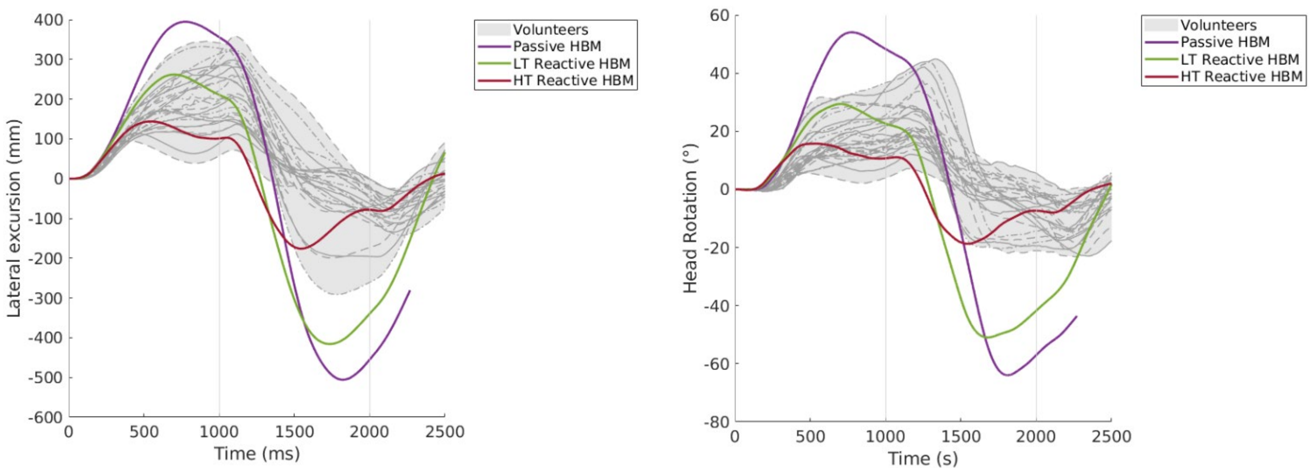

(a) Head lateral excursion. (b) Head lateral bending.

Fig. 6. Head lateral excursion and lateral bending of the passive and reactive muscle controls with two muscle states compared to the sled volunteer experiments without lateral structure from Sandoz *et al.* [9].

The maximum lateral excursion of the head for the volunteers during the acceleration phase on the sled without the lateral structure varies between 94 mm and 357 mm (Fig. 6(a)). The lateral excursion of the passive HBM extends beyond the corridor, achieving a maximum head displacement of 394 mm. The lateral displacement of the head in case of the *low tensed* and *highly tensed* AHBMs falls within the corridor, reaching a maximum excursion of 262 mm and 144 mm, respectively. The maximum lateral head excursion of the *low tensed* model is 95 mm below the maximum volunteer excursion, yet it is above the maximum average excursion of 224 mm. During the deceleration phase only the *highly tensed* reactive model is capable of showing a similar kinematic trend as the volunteers.

The head lateral bending exhibited by the volunteers ranged from 5° to 44° (Fig. 6(b)). The passive HBM sustained a maximum lateral bending of 54° during the acceleration phase. The application of the reactive muscle control with the *low tensed* and *highly tensed* activation levels resulted in a reduction of the lateral bending of the head to 29° and 15°, respectively. The *highly tensed* model shows a lateral bending similar to that of the volunteers demonstrating less lateral rotation, while the *low tensed* model displayed comparable kinematics to those volunteers exhibiting larger rotations during the initial 500 ms of the acceleration phase. However, from that point onward, the volunteers continued to rotate their heads, whereas the *low tensed* model reacted by rotating the head towards its initial position.

Similar to the head lateral excursion during the deceleration phase, it is observed that only the *highly tensed* reactive HBM shows a head lateral bending that is comparable to those measured among the volunteers.

Figure 7 shows the comparison between the kinematics of the volunteers and the HBMs for those configurations with the lateral structure positioned to the right-hand side of the volunteers. Furthermore, two distinct volunteer corridors are presented, displaying the response of the volunteers for two muscular states: relaxed and braced. These two behaviours are represented by the shaded areas in grey and light blue, respectively. It is noteworthy that the passive and reactive HBM curves are identical to those displayed in Fig. 6; in this instance, however, they are compared with the volunteers' corridor from the configuration with the lateral structure, which has been demonstrated to limit the lateral excursion and rotation of the head [26].

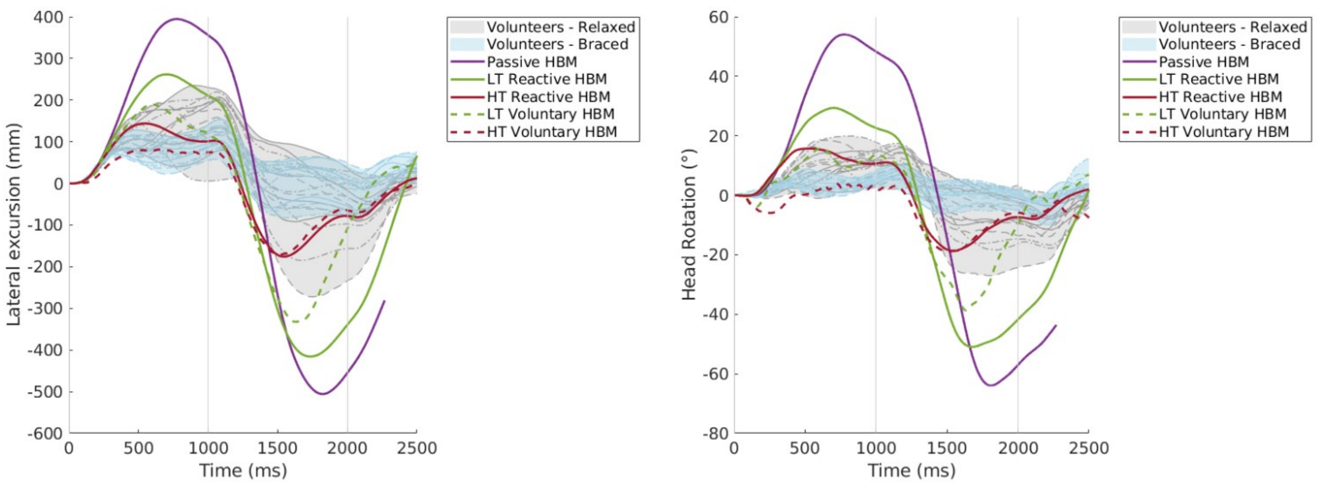

(a) Head lateral excursion. (b) Head lateral bending.

Fig. 7. Head lateral excursion and lateral bending of the reactive and voluntary muscle controls with two muscle states compared to the sled volunteer experiments with lateral structure from González-García *et al*. [26].

The passive HBM maximum head lateral excursion exceeds the maximum lateral excursion of the relaxed volunteers by 160 mm during the acceleration phase (Fig. 7(a)). The *low tensed* model with the reactive muscle control also exceeds the maximum lateral excursion by 25 mm (Fig. 7(a)), while it fell within the corridor when compared to the response of the volunteers without the lateral structure (Fig. 6(a)). The application of the voluntary muscle control to the *low tensed* model reduces the head lateral displacement by 71 mm, reaching a maximum head lateral excursion of 261 mm and 190 mm for the reactive and voluntary muscle controls, respectively. The maximum head lateral excursion among the volunteers is 235 mm during the relaxed muscle state configuration. The application of the voluntary muscle control to the *highly tensed* model reduces its maximum head lateral displacement from 143 mm to 79 mm during the acceleration phase. The head displacement of the *highly tensed* model is comparable to that of the braced volunteers.

Similarly, the passive HBM and the *low tensed* reactive HBM are not capable of representing the lateral bending of the head of the volunteers on the sled with the structure placed to their right-hand side (Fig. 7(b)). The head lateral bending of these two models is 54° and 29°, respectively, in comparison to a maximum lateral bending of 19° for the relaxed volunteers. The application of the voluntary muscle control reduces the maximum lateral bending to 15° for the *low tensed* model, which is representative of the volunteers exhibiting greater head lateral bending. In the case of the *highly tensed* model, the maximum head lateral bending during the acceleration phase is reduced from 15° to 4° for the reactive and voluntary HBM, respectively. The head lateral bending for the volunteers during the configurations with braced muscles ranges between 1° and 10°. Consequently, the *highly tensed* model with the voluntary muscle control demonstrates comparable kinematics during the acceleration phase. However, only the *highly tensed* model, irrespective of the applied muscle control, is capable of exhibiting comparable kinematics to the volunteers during the deceleration phase.

The kinematic sequence of the five models is illustrated in Fig. 8 in time intervals of 250 ms up to a total of 2000 ms. As demonstrated by the curves in Fig. 6 and Fig. 7, the passive HBM displays excessive upper-body excursion and rotation (Fig. 8(a)). Both mentioned measurements are reduced in the case of the reactive HBMs compared with the passive HBM. Finally, an inward lateral bending of the head can be observed for the voluntary AHBMs, when approaching the lateral structure between 500 ms and 750 ms.

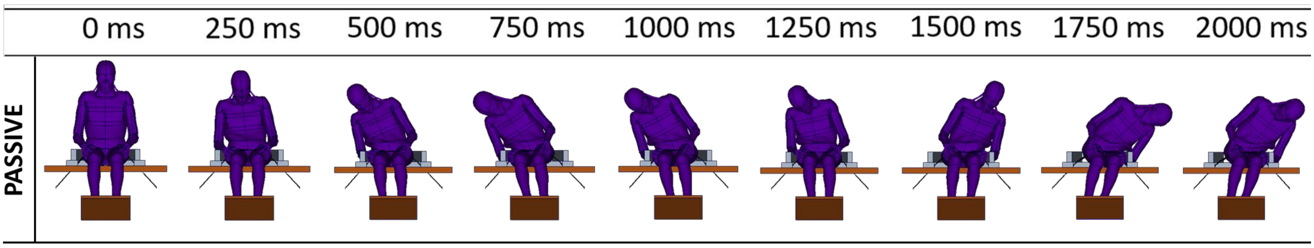

(a) Passive HBM.

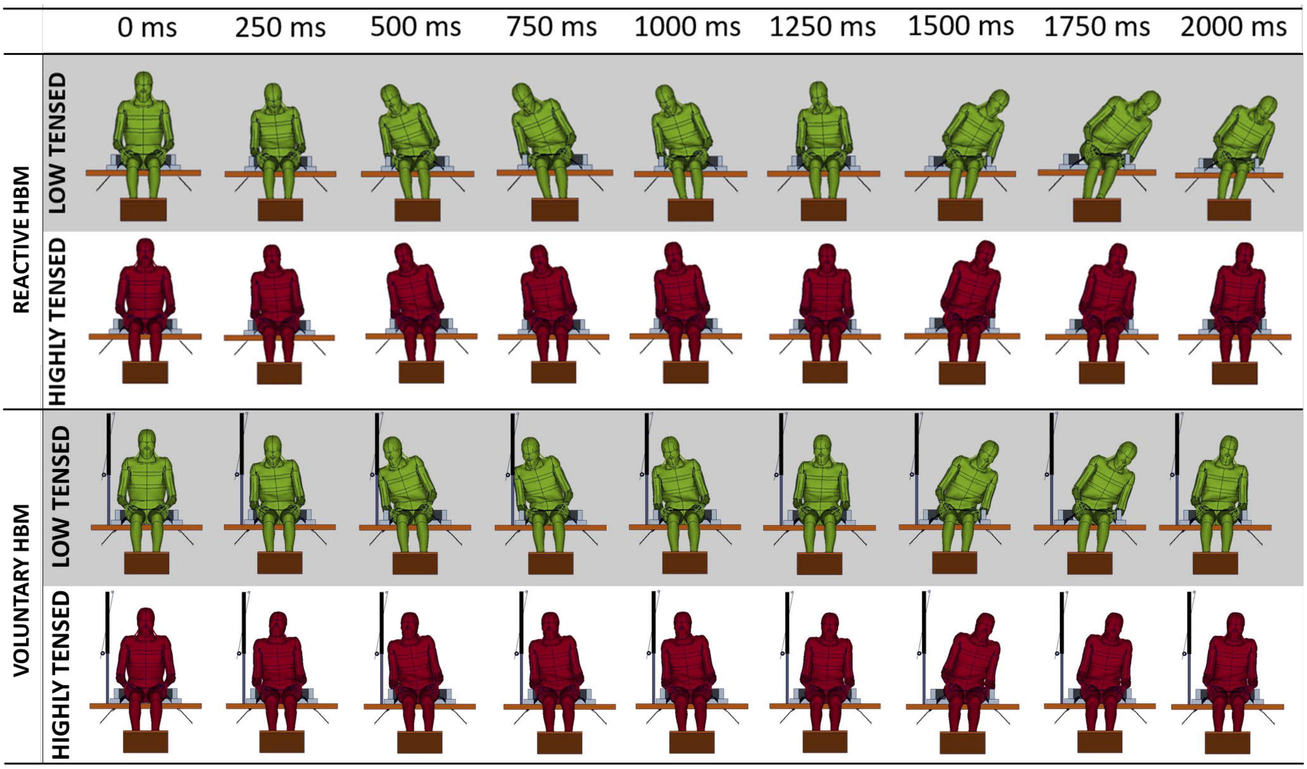

(b) Reactive and voluntary AHBM for two muscle states.

Fig. 8. Kinematic sequence of the THUMS TUC-VW HBM passive, reactive and voluntary muscle control under lateral acceleration with and without lateral structure from the experiments by González-García et al. [26].

IV. DISCUSSION

Previous researchers [23-25] have hypothesised, based on results from volunteer experiments, that vehicle occupants perform protective movements during, for example, lane-changing manoeuvres to try to avoid contact with the structure of the vehicle. Some of the arguments to support this assumption are the non-symmetrical excursion during right and left lane changes [25] or the difference in maximum head lateral excursion in different vehicle types, being more reduced in smaller vehicles [23]. Furthermore, it has been observed that in volunteer experiments on a sled, where typically there is no lateral structure on their side, volunteers show a pendulum-like movement of the upper-body [37], whereas volunteers in vehicle experiments tend to laterally bend their head inward when moving towards the vehicle structure [6][38]. Further volunteer experiments were performed on a sled with and without a lateral structure on the side of the volunteers and it was demonstrated that the head excursion and lateral bending varied depending on the surrounding environment [26]. Additionally, the head excursion of the volunteers generally reaches a steady position during braking pulses, whereas for the majority of the volunteers the flexion of the head diminishes during the same pulse [39], which suggests a voluntary extension of the neck.

It is important to estimate accurately enough the posture of the AHBMs at the end of the pre-crash phase, since this will facilitate a better understanding of the injuries during the subsequent collision. Moreover, an AHBM with an accurate prediction of the kinematics can serve as a tool to improve and develop new safety systems considering the accelerations occurring during pre-crash manoeuvres.

Most of the currently available AHBMs have been validated using experimental data from the aforementioned publications. Although some of them are capable of performing some voluntary tasks, such as exerting forces to the steering wheel and brake pedal [15-17], to the authors' knowledge none of them has the capacity to perform voluntary head-neck movements during avoidance manoeuvres.

Therefore, this study aimed to enhance the HBM muscle control to enable head-neck voluntary movements, previously reported in the literature, in order to better predict the kinematics of the occupants during pre-crash manoeuvres. To exercise the development of the muscle control algorithm, the 50th percentile male THUMS TUC-VW AHBM was chosen. The kinematics of the model using the passive version, and two different controllers – one with reactive muscle control and the other with additional voluntary muscle control features – were compared against experimental data obtained from volunteers experiencing a braking pulse [4] and a lateral acceleration [9][26]. Moreover, for those simulations including muscle control, two different levels of activation, namely *low tensed* and *highly tensed*, were analysed. The purpose of the two different muscle activation levels is to represent the volunteers exhibiting larger and shorter excursions, which in turn correspond with lower and higher muscle activation levels, respectively.

The kinematic curves of the passive HBM fall outside the corridor of the volunteers, except for the thoracic excursion during the braking pulse. The thoracic excursion is mainly limited by the shoulder seat-belt and therefore it does not allow any further forward excursion of the model. The passive HBM, unlike the volunteers, does not respond to the external forces and therefore has no muscle activation. It is therefore intended that this model will exhibit greater excursions than those exhibited by the volunteers.

The reactive HBM is able to reproduce the forward excursion during the braking pulse as well as the lateral excursions during the acceleration phase for the configuration without lateral structure. However, this model fails to reproduce the flexion of the head during the braking pulse as well as to mimic the kinematics of the volunteers during the lateral acceleration when the lateral structure was placed to the right-hand side.

Finally, the voluntary HBM significantly improves the head flexion of the HBM during the braking pulse for the *low tensed* muscle activation by initiating the control of the voluntary neck extension. Moreover, the lateral bending controller improves the performance of the HBM subjected to the lateral acceleration with the lateral structure. However, only the *highly tensed* HBM is capable of reproducing kinematics comparable to those exhibited by the relaxed volunteers during the deceleration phase of the pulse. None of the presented muscle control algorithms is capable of simulating the kinematics of the braced volunteers during the deceleration phase of the lateral pulse. The authors hypothesise that further voluntary movements can be identified during the deceleration phase and together with greater co-contraction of the antagonist muscles could improve the performance and stabilisation of the AHBM during this phase.

Future work will focus on the implementation of the muscle control algorithm to a 5th percentile female HBM, including its validation using experimental data acquired with female volunteers.

V. CONCLUSION

The implementation of a novel voluntary head-neck muscle control algorithm into an AHBM yields more accurate predictions of kinematics during braking and lateral manoeuvres than the reactive AHBM, as evidenced by the comparison with the volunteer experimental responses. The muscle control algorithm considers input variables representing the visual, vestibular and proprioceptive systems. In particular, during lateral accelerations the model is capable of reacting differently depending on the proximity of its head to the surrounding environment. This enables the AHBM to demonstrate an inward rotation of the head, comparable to those observed in in-vehicle volunteer experiments. It is also able to represent volunteers exhibiting varying degrees of muscle activation. Moreover, it is not necessary to calibrate the muscle controller parameters for each load case. These parameters remain valid for multidirectional loading, as the muscle control relies on the lengthening of the muscles. Lastly, the parameters of voluntary muscle control do not require calibration for varying load levels or different vehicle types. This is due to the fact that the muscle activation levels are determined by the firing rate of neurons, which, in turn, is solely dependent on the movement of the HBM and its distance to the surrounding structures.

VI. REFERENCES

[1] González-García, M., Weber, J., Peldschus, S. (2021) Potential effect of pre-activated muscles under a far-side lateral impact. *Traffic Injury Prevention,* **vol. sup1**(22): pp. 148–152.

[2] González-García, M., Weber, J., Peldschus, S. (2020) Numerical Study to Quantify the Potential Influence of Pre-Activated Muscles during the In-Crash Phase. In: *International Symposium: Human Modeling and Simulation in Automotive Engineering*.

[3] Östh, J., Larsson, E., Jakobsson, L. (2022) Human Body Model Muscle Activation Influence on Crash Response. *Proceedings of the IRCOBI Conference*, 2022, Porto, Portugal.

[4] Huber, P., Kirschbichler, S., Prüggler, A., Steidl, T. (2015) Passenger kinematics in braking, lane change and oblique driving maneuvers. *Proceedings of the IRCOBI Conference*, 2015, Lyon, France.

[5] Östh, J., Davidsson, J., Brolin, K. (2013) Driver Kinematic and Muscle Responses in Braking Events with Standard and Reversible Pre-tensioned Restraints: Validation Data for Human Models. *Stapp Car Crash Journal,* **57**: pp. 1–41.

[6] Ghaffari, G., Brolin, K., *et al*. (2018) Passenger kinematics in Lane change and Lane change with Braking Manoeuvres using two belt configurations: standard and reversible pre-tensioner. *Proceedings of the IRCOBI Conference*, 2018, Athens, Greece.

[7] Chan, H., Albert, D. L., Gayzik, F. S., Kemper, A. R. (2023) Occupant Kinetics and Muscle Responses of Relaxed and Braced Small Female and Mid-Size Male Volunteers in Low-Speed Frontal Sled Tests. *SAE International Journal of Transportation Safety*.

[8] Beeman, S., Kemper, A., Madigan, M., Duma, S. (2011) Effects of bracing on human kinematics in low-speed frontal sled tests. *Annals of Biomedical Engineering,* **12**(39): pp. 2998–3010.

[9] Sandoz, B., Persohn, S., González-García, M., Weber, J. (2023) Upper body behaviour of seated humans in vivo under controlled lateral accelerations. *Clinical Biomechanics,* **105**.

[10] Ejima, S., Ono, K., Holcome, S., Kaneoka, K., Fukushima, M. (2007) A Study on Occupant Kinematics Behaviour and Muscle Activities during Pre-Impact Braking Based on Volunteer Tests. *Proceedings of the IRCOBI Conference*, 2007, Maastricht, the Netherlands.

[11] Ólafsdóttir, J., Östh, J., Brolin, K. (2019) Modelling Reflex Recruitment of Neck Muscles in a Finite Element Human Body Model for Simulating Omnidirectional Head Kinematics. *Proceedings of the IRCOBI Conference*, 2019, Florence, Italy.

[12] Yigit, E. (2018) Reaktives FE-menschmodell im insassenschutz. Wiesbaden: Springer Fachmedien.

[13] Putra, I. and Thomson, R. (2022) Analysis of control strategies for VIVA OpenHBM with active reflexive neck muscles. *Biomechanics and Modeling in Mechanobiology,* **6**(21): pp. 1731–1742.

[14] Martynenko, O., Neininger, F., Schmitt, S. (2019) Development of a Hybrid Muscle Controller for an Active Human Body Model in LS-Dyna Capable of Occupant Kinematics Prediction in Frontal and Lateral Maneuvers. In: *International Technical Conference on the Enhanced Safety of Vehicles*, 2019, Eindhoven, the Netherlands.

[15] Kato, D., Nakahira, Y., Atsumi, N., Iwamoto, M. (2018) Development of Human Body Model THUMS Version 6 containing Muscle Controllers and Application to Injury Analysis in Frontal Collision after Brake Deceleration. *Proceedings of the IRCOBI Conference*, 2018, Athens, Greece.

[16] Devane, K., Chan, H., Albert, D., Kemper, A., Gayzik, F.S (2022) Implementation and calibration of active small female and average male human body models using low-speed frontal sled tests. *Traffic Injury Prevention*, **vol sup1**(23): pp. 44–49.

[17] Devane, K., Chan, H., Albert, D., Kemper, A., Gayzik, F.S (2023) Response of small female and midsize male models with active musculature in pre-crash maneuvers and low-speed impacts. *Traffic Injury Prevention*, **vol sup1**(24): pp. 9–15.

[18] Correia, M.A., McLachlin, S.D., Cronin, D.S. (2021) Vestibulocollic and Cervicocollic Muscle Reflexes in a Finite Element Neck Model During Multidirectional Impacts. *Annals of Biomedical Engineering*, **49**: pp. 1645–1656.

[19] Larsson, E., Iraeus, J., *et al*. (2019) Active Human Body Model Predictions Compared to Volunteer Response in Experiments with Braking, Lane Change, and Combined Manoeuvres. *Proceedings of the IRCOBI Conference*, 2019, Florence, Italy.

[20] Wochner, I., Nölle, L., Martynenko, O., Schmitt, S. (2022) “Falling heads": investigating reflexive responses to head-neck perturbations. *BioMedical Engineering Online,* **21**.

[21] Martynenko, O., Wochner, I., *et al*. (2021) Comparison of the Head-Neck Kinematics of Different Active Human Body Models with Experimental Data. *Proceedings of the IRCOBI Conference*, 2021, Online.

[22] Iwamoto, M., Nakahira, Y., *et al*. (2007) Development of advanced human models in THUMS. In: *6th European LS-Dyna Users' Conference*, 2007, Gothenburg, Sweden.

[23] Reed, M., Ebert, S., Jones, M., Park, B.-K. (2021) Occupant Dynamics During Crash Avoidance Maneuvers (Report No. DOT HS 812 997). National Highway Traffic Safety Administration.

[24] Peldschus, S., Davidsson, J., Klug, C., Dussinger, S., Schießler, M. (2021) Standardised validation procedure for qualifying the HBM to be used for assessing effectiveness of pilot protection principles. Deliverable D5.2, OSCCAR Project; Grant Agreement No. 768947, 2021.

[25] Kirschbichler, S., Klein, C., *et al.* (2023) Passenger Kinematics in Reclined Sitting Position in Braking and Steering Manoeuvres. *Proceedings of the IRCOBI Conference*, 2023, Cambridge, UK.

[26] González-García, M., Peldschus, S., Weber, J., Persohn, S., Sandoz, B. (2024) Influence of the surrounding environment on the response of seated midsize male volunteers subjected to lateral sled accelerations. *Journal of Biomechanics,* **177**.

[27] Davidsson, J. (2021) Validated and computationally robust active HBMs. Deliverable D3.2, OSCCAR Project; Grant Agreement No. 768947, 2021.

[28] Song, B., Chen, W., Ge, Y., Weerasooriya,. T. (2007) Dynamic and quasistatic compressive response of porcine muscle. *Journal of Biomechanics,* **40**(13): pp. 2999–3005.

[29] Nie, X., Cheng, J., Chen, W., Weerasooriya, T. (2010) Dynamic tensile response of porcine muscle. *Journal of Applied Mechanics,* **78**(2).

[30] Mattucci, S., Moulton, J., Chandrashekar, N., Cronin, D. (2012) Strain rate dependent properties of younger human cervical spine ligaments. *Journal of the Mecahncial Behavior of Biomedical Materials,* **10**: pp. 216–226,.

[31] Van Loocke, M., Lyons, C., Simms, C. (2008) Viscoelastic properties of passive skeletal muscle in compression: stress-relaxation behavior and constitutive modelling. *Journal of Biomechanics,* **41**(7): pp. 1555–1156.

[32] Günther, M. and Ruder, H. (2003) Synthesis of two-dimensional human walking: A test of the lambda-model. *Biological cybernetics,* **89**: pp. 89–106.

[33] Hatze, H. (1977) Biological cybernetics - a myocybernetic control model of skeletal muscle. *Biological Cybernetics,* **25**: pp. 103–119.

[34] Meijer, R., Elrofai, H., Broos, J., van Hassel, E. (2013) Evaluation of an active multi-body human model for braking and frontal crash events. *Proceedings of the IRCOBI Conference*, 2013, Gothenburg, Sweden.

[35] Dayan, P. and Abbott, L. F. (2001) *Theoretical Neuroscience: Computational and Mathematical Modeling of Neural Systems*. The MIT Press, 2001.

[36] Kofler, D., Heider, E., *et al*. (2022) Precooni & OM4IS Seat Model [Online]. Available: https://openvt.eu/osccar/precrash_seat_models/precooni-om4is.

[37] Ejima, S., Ito, D., *et al*. (2012) Effects of Pre-impact Swerving/Steering on Physical Motion of the Volunteer in the Low-Speed Side-Impact Sled Test *Proceedings of the IRCOBI Conference*, 2012, Dublin, Ireland.

[38] Muggenthaler, H., Adamec, J., Praxl, N., Schönpflug, M. (2005) The Influence of Muscle Activity on Occupant Kinematics. *Proceedings of the IRCOBI Conference*, 2005, Prague, Czech Republic.

[39] Kirschbichler, S., Klein, C., Klug, C., Kofler, D. (2021) Precooni & OM4IS Data [Data set], Zenodo.

VII. APPENDIX

A. *Additional Simulation Results – Braking Load Case*

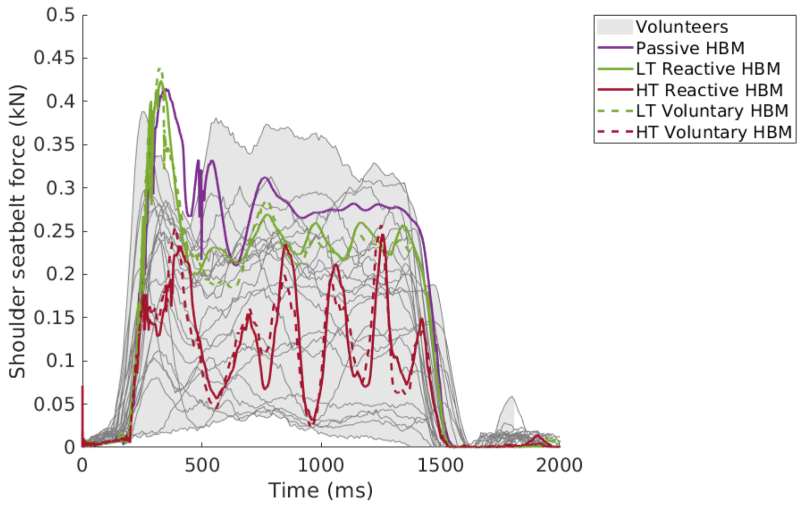

Fig. A1. Shoulder seat-belt force for the simulation with the passive, reactive and voluntary muscle controls with two muscle states compared to the validation data from Huber *et al*. [4][39].

B. Additional Simulation Results – Lateral Acceleration Load Case

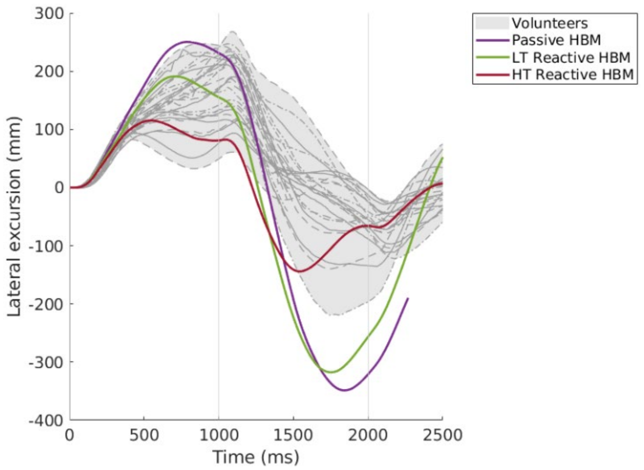

(a) First thoracic vertebra lateral excursion.

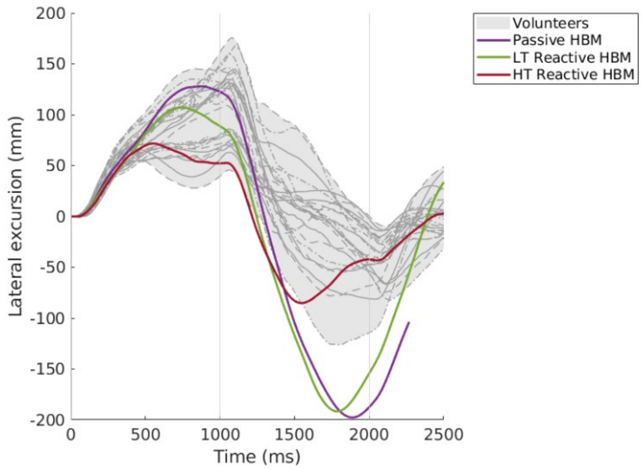

(b) Eighth thoracic vertebra lateral excursion.

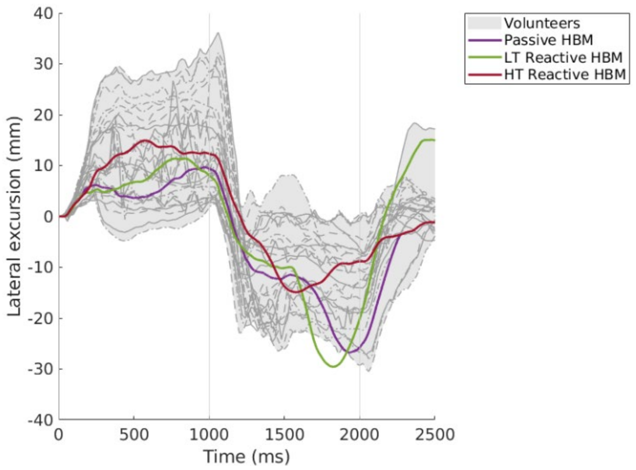

(c) Sacrum lateral excursion.

Fig. B1. T1, T8 and sacrum lateral excursion of the passive and reactive muscle controls with two muscle states compared to the sled volunteer experiments without lateral structure from Sandoz *et al.* [9].

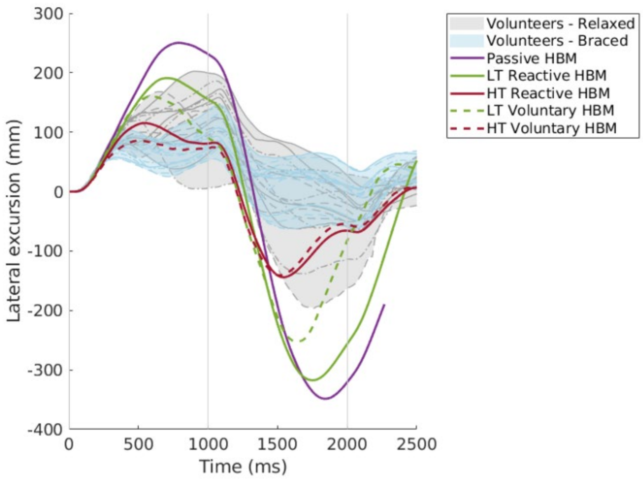

(a) First thoracic vertebra lateral excursion.

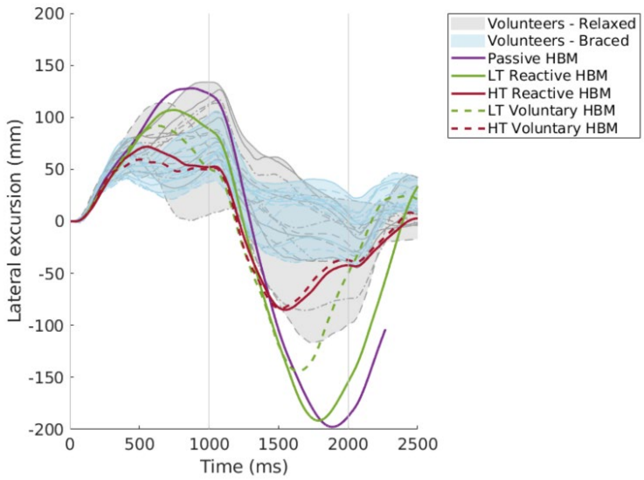

(b) Eighth thoracic vertebra lateral excursion.

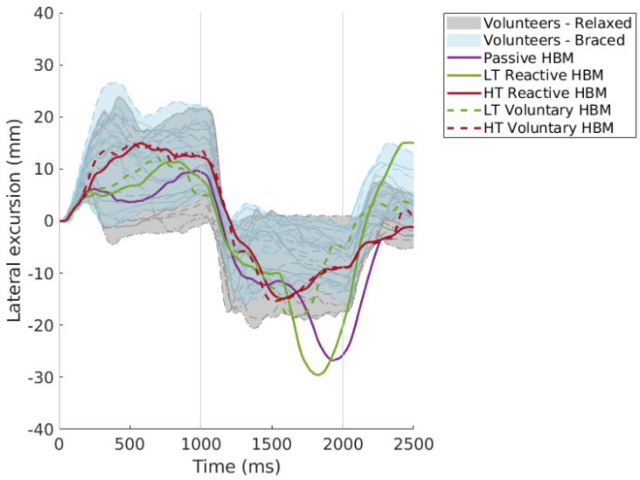

(c) Sacrum lateral excursion.

Fig. B2. T1, T8 and sacrum lateral excursion of the reactive and voluntary muscle controls with two muscle states compared to the sled volunteer experiments with lateral structure from González-García *et al.* [26].

C. Clustering scheme for neck muscle control

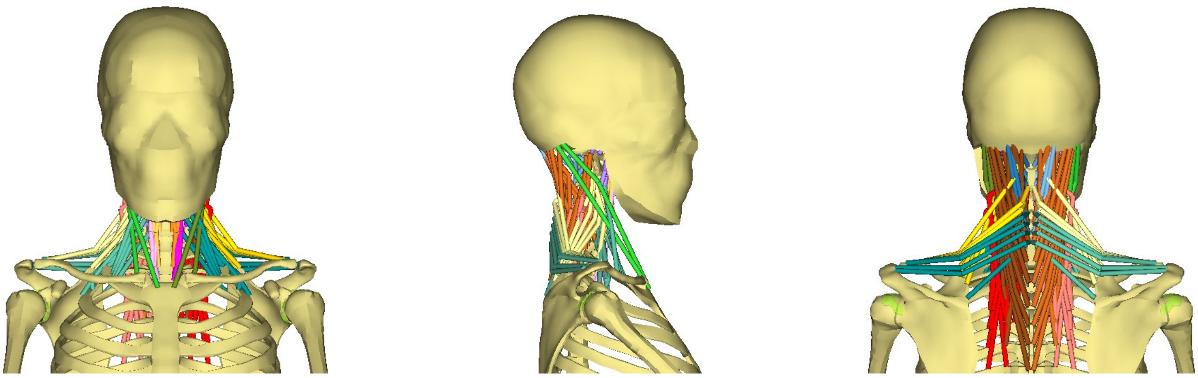

(a) Anterior view (b) Side view (c) Posterior view

Fig. C1. Clustering scheme applied to the 18 controllers of the neck muscles.